Ultrasound-induced inertial cavitation from gas-stabilizing nanoparticles

J. J. Kwan, S. Graham, R. Myers, R. Carlisle, E. Stride, and C. C. Coussios*
Institute of Biomedical Engineering, University of Oxford, Oxford OX3 7DQ, United Kingdom
(Received 8 March 2015; published 19 August 2015)

The understanding of cavitation from nanoparticles has been hindered by the inability to control nanobubble size. We present a method to manufacture nanoparticles with a tunable single hemispherical depression (nanocups) of mean diameter 90, 260, or 650 nm entrapping a nanobubble. A modified Rayleigh-Plesset crevice model predicts the inertial cavitation threshold as a function of cavity size and frequency, and is verified experimentally. The ability to tune cavitation nanonuclei and predict their behavior will be useful for applications ranging from cancer therapy to ultrasonic cleaning.

DOI: 10.1103/PhysRevE.92.023019 PACS number(s): 82.70.Dd, 43.25.Yw, 47.55.dp, 81.07.−b

I. INTRODUCTION

Microbubbles undergo violent collapse when exposed to sufficiently large acoustic rarefactional pressure amplitudes. This phenomenon, known as inertial cavitation [1], results in shock-wave generation, broadband acoustic emissions [2], jetting [3], and microstreaming [2], and has been identified as a key mechanical trigger for various medical [4,5] and industrial applications [6,7]. Microbubbles are suboptimal cavitation nuclei in certain applications due to size-related limitations and their rapid depletion. For example, microbubbles are limited by their confinement to the vasculature and their short-lived cavitation activity (<2 min [8]) reducing their capacity to mediate delivery of a therapeutic. Thus, researchers have sought to develop nanosized particles, such as nanoemulsions [9], nanobubbles [10], and mesoporous solid nanoparticles [11] that are able to nucleate cavitation upon exposure to ultrasound.

Solid submicrometer-sized particles reduce the cavitation threshold of water [12,13]. Yet little is known about the cavitation behavior of nanoparticle systems. Despite its critical importance, the influence of cavity size on the inertial cavitation threshold and its comparison to theoretical predictions have not been characterized. Our aim in this paper is to (1) hypothesize a mechanism for inertial cavitation nucleated from a nanoparticle and predict inertial cavitation thresholds, (2) develop a nanoparticle with a size-tunable hemispherical cavity that is capable of trapping gas (henceforth referred to as a nanocup), and (3) compare experimentally determined inertial cavitation thresholds from nanocups with the theoretical predictions.

II. THEORY

Previous work has shown that surfaces that trap gas within a nanoscale crevice are capable of generating a cavitation bubble after exposure to a shock wave [14]. Inertial cavitation from nanobubbles trapped on solid nanoparticles with single cavities upon exposure to ultrasound fields with pressure amplitudes near 1 MPa has not been previously theoretically or experimentally demonstrated to our knowledge. Unlike bubbles on planar surfaces, bubbles formed on nanoparticles cannot expand onto the surface beyond the crevice indefinitely. We therefore propose that the mechanism for inertial cavitation on gas-trapping nanocups is that the inertia of the surrounding liquid causes necking and detachment of the gas cavity during the negative half cycle of the ultrasound wave, allowing for inertial growth and collapse during the positive half cycle (Fig. 1). A modified crevice model is necessary to capture these dynamics. Assuming a hemispherical geometry, we applied a Rayleigh-Plesset crevice model [15,16] to calculate the size and position of the bubble wall, defined as $R\ddot{R} + (3/2)\dot{R}^2 = (1/\rho_L)[P_L(R) - P_{ac}(t) - P_H]$ where R, $\dot{R}$, and $\ddot{R}$ are the size, velocity, and acceleration of the radius of curvature for the bubble wall, ρ_L is the density of water, P_L is the liquid pressure at the bubble wall, P_{ac} is the acoustic pressure, t is time, and P_H is the hydrostatic pressure, 101 kPa. The liquid pressure at the bubble wall is

$$P_L = P_{B_0}\left(\frac{V}{V_0}\right)^{-k} - \frac{2\sigma}{R} - \frac{4\mu_L}{R}\dot{R}$$

where P_{B_0} and V_0 are the initial bubble pressure and volume respectively, V is the instantaneous bubble volume, the polytropic gas constant $k = 1.4$, the surface tension $\sigma = 73\,\mathrm{mN\,m^{-1}}$, and the liquid viscosity $\mu_L = 0.89\,\mathrm{mPa\,s}$. We considered three stages of bubble evolution: (1) the bubble is cavity constrained, (2) it is pinned to the cavity opening, and (3) it is detached from the cavity [16]. We assumed that the bubble detaches from the cavity if the contact angle drops below the receding contact angle (52°) [17]. Based on the geometry of the nanocup, R is defined as follows for each of stages:

$$R = \begin{cases} [(x-h)^2 + w(x)^2]^{1/2} & (1)\ h = \text{const (inside the cavity)}, \\ [(L-h)^2 + w(L)^2]^{1/2} & (2)\ h = \text{variable (surface of cavity)}, \\ R & (3)\ \text{free bubble}, \end{cases} \quad (1)$$

where x is the height of the three-phase contact point, h is the distance between the center of the bubble and the bottom edge of the cavity, $w(x) = [x(2r_C - x)]^{1/2}$ is the bubble contact width, r_C is the cavity radius, and L is the cavity length (Fig. 1).

Here the inertial cavitation threshold is defined as the minimum peak rarefactional pressure (PRP) amplitude for which the bubble wall speed equals or exceeds the speed of sound in the liquid [18] during the compressional phase of

*Corresponding author: constantin.coussios@eng.ox.ac.uk

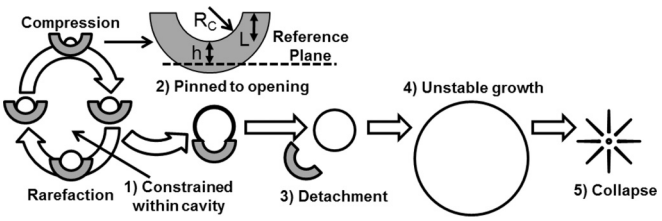

FIG. 1. Hypothesis of inertial cavitation nucleated from a nanocup and schematic of a nanocup.

the ultrasound. This is experimentally equivalent to the generation of broadband acoustic emissions remotely detectable by a passive cavitation detector (PCD) of center frequency and bandwidth at least five times greater than the incident ultrasound pulse. Below the inertial cavitation threshold, the model predicts that a bubble trapped within a nanoscale hemispherical cavity gently oscillates without detaching. Above the inertial cavitation threshold, we predict that the nanobubble detaches, inertially grows, and collapses during the positive pressure phase.

We determined the inertial cavitation threshold, namely the pressure amplitude at which $\dot{R} > c_L$, where c_L is the speed of sound in the liquid, with the Rayleigh-Plesset crevice model. Inertial cavitation thresholds were determined as a function of cavity diameter for two excitation frequencies (Fig. 2). Lower frequencies have a longer half period of rarefaction. This allows a nanobubble from a given initial cavity size to expand to a correspondingly larger size prior to the compressional half cycle, increasing the likelihood of inertial collapse [19]. The inertial cavitation threshold will thus decrease with decreasing excitation frequency for a given cavity diameter.

III. EXPERIMENTAL VERIFICATION

A. Tuning of nanocups

To verify the predicted inertial cavitation threshold as a function of cavity size, we first developed a protocol for fabricating nanocups in three tightly controlled size ranges. This was achieved by modifying a seeded polymerization technique [20], apparently not previously used to produce either

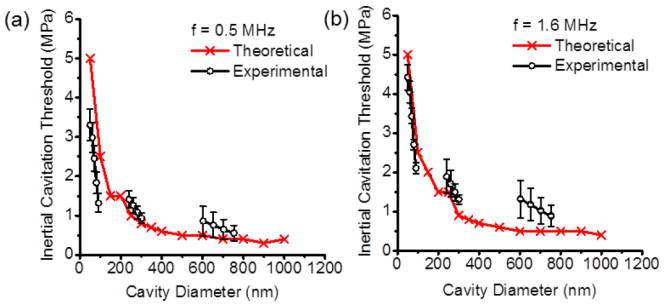

FIG. 2. (Color online) Inertial cavitation thresholds predicted numerically and determined experimentally at (a) 0.5 MHz and (b) 1.6 MHz. Experimentally determined inertial cavitation thresholds are shown to agree with predicted values. Each experimental point represents the mean and standard deviation across three measurements.

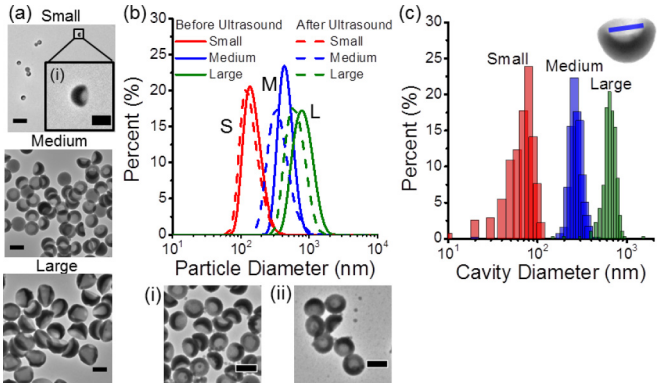

FIG. 3. (Color online) (a) TEM images of small, medium, and large nanocups. The scale bars represent 500 nm. The inset TEM image (i) is a single small nanocup (scale bar represents 200 nm). (b) Size measurements of small (S), medium (M), and large (L) nanocups before and after ultrasound exposure. The TEM images below the graph show medium nanocups before (i) and after (ii) ultrasound exposure. The scale bars represent 500 nm. (c) Size distributions of cavity sizes of nanocups measured from TEM images. An image of a single nanocup is shown in the inset of the figure with a blue line indicating the size of the cavity measured.

nanocups or ultrasound-responsive gas-entrapping nanoparticles. Briefly, we coated three differently sized (100, 300, and 460 nm) polystyrene nanospheres (10 wt %) with a copolymer of methyl methacrylate, 2-hydroxymethyl methacrylate, and a divinylbenzene (80 vol %) cross-linker in a 10:1:6 vol/vol/vol ratio at 80 °C. The reaction was initiated with potassium persulfate at 3.5 mg/ml. All chemicals were purchased from Sigma-Aldrich and used without further purification.

The polymer coating induced a swelling of the polystyrene bead allowing for a void to form in the center of the nanoparticle [21,22], which subsequently deformed and created a uniform 'cup' shaped depression on the surface as seen in transmission electron microscopy (TEM; Hitachi H-7650) images [Fig. 3(a)]. This depression enabled stabilization of gas after air drying and resuspension of nanocups in ultrapure water, yielding a narrow size distribution [Fig. 3(b)] as measured by dynamic light scattering (DLS; ZetaSizerNano, Malvern). We manufactured three distinct diameter ranges of nanocups: small (170 nm), medium (480 nm), and large (790 nm). Typically, the particle concentrations were measured between 10^9 and 10^{11} particles/ml using a Coulter counter (Qnano, Izon), and were later diluted to between 10^9 and 10^{10} particles/ml for acoustic characterization. All nanocups carried negative surface charge in the range -15 to -46 mV as measured by the ZetaSizerNano, and demonstrated no aggregation in any experiment. We report here the concept of utilizing a single cavity on a nanoparticle to trap gas as a cavitation nucleus and its subsequent manufacturing and air drying methodology.

B. Cavitation measurements of nanocups

The inertial cavitation threshold was determined experimentally for each nanocup size range at both 0.5 and 1.6 MHz, and superimposed onto the theoretically predicted threshold (Fig. 2). Nanocups were made to flow continuously inside a

hollow microfiber (Cuprophan, Membrana) with an acoustic sample volume of 0.02 µl to enable sample replenishment in the ultrasound exposure region. Ultrasound excitation was provided by a single-element ultrasound transducer (Sonic Concepts H107) placed in a water bath [23,24] orthogonal to the microfiber and driven at either the fundamental or the third harmonic. All acoustic pressures reported are PRP measured using a 0.4-mm-diameter needle hydrophone (ONDA 1056, Onda Corporation).

A PCD (V319-SU, 15 MHz PZT, Panametrics) of frequency at least five times the main ultrasound excitation was used to record acoustic emissions from the nanocups during exposure to ultrasound over a range of acoustic amplitudes. We conducted 200 single ten-cycle-burst ultrasound measurements for each nanocup population. A 2 MHz high-pass filter was applied to remove reflections of the incident ultrasound beam from to the sample holder. The received signal was further processed to obtain the power spectral density and associated power of the acoustic signal. The inertial cavitation threshold of pure degassed water has previously been reported to be in excess of 30 MPa [25], a pressure amplitude not achievable with our experimental setup. Water used in our experiments was obtained from a water filtration system (Milli-Q, Merck Millipore) that passes de-ionized water through a 220 nm filter, resulting in ultrapure water. We observed no cavitation events in pure water across all frequencies and pressures studied; any signal detected above background is solely from nanocup-induced cavitation.

Below the inertial cavitation threshold of nanocups no signal was detected by the PCD. Whenever a signal was detected by the PCD, it was purely broadband in nature. An inertial cavitation event is defined as an increase in broadband power greater than 10 dB [26]. Harmonic emissions, which are indicative of stable cavitation that are typically observed from microbubbles [26], were never detected [Fig. 4(a)]. Nanocups thus appear to exclusively nucleate inertial cavitation [2]. Although previous modeling work has demonstrated that broadband emissions are also caused by temporal fluctuations in the number of bubbles over a large volume [27], the focal volume of the PCD in the present work is too small (<200 µm) to detect more than a few bubbles cavitating simultaneously. Therefore fluctuations in the number of bubbles are unlikely to be the source of the detected broadband noise.

We propose that only broadband emissions are observed because the driving frequencies are far below the resonance frequencies of the nanobubbles, which are estimated to be on the order of 10 MHz (1 µm cavity diameter) and as high as 120 MHz (100 nm cavity diameter). This is confirmed by the model, which shows that the inertia of the surrounding liquid required to detach a nanobubble from the nanocup always induces a violent collapse.

Nanocups and associated cavity sizes have a very narrow size distribution. Larger cavities will nucleate a bubble at lower pressures (Fig. 2). Consequently there is a corresponding range of pressures over which inertial cavitation is expected to be observed. Thus the probability of inertial cavitation increases monotonically with increasing pressure and is a function of both frequency and the cavity size distribution of the sample. This probability of cavitation is measured experimentally as the percentage of ultrasound pulses that yields a measurable inertial cavitation event for a given pressure amplitude, depicted in Fig. 4(b). In order to enable a direct comparison between the experimentally measured probability of inertial cavitation and the theoretically determined inertial cavitation threshold of the nanocups, we assume that the probability of inertial cavitation is directly proportional to the likelihood of a suitably sized cavity being present in the ultrasound field. Thus, an experimentally measured probability of cavitation of 50% at a certain acoustic pressure implies that, at that pressure, 50% of particles in the size distribution [Fig. 3(b)] have a cavity of the right size [Fig. 3(c)] to cavitate inertially. For example, at 1.5 MPa the probability of inducing inertial cavitation across 200 pulses at 0.5 MHz for the medium-sized particles is found experimentally to be 0.75. Looking at the cavity size distribution of Fig. 3(c) for the medium-sized particles, and starting with the largest size, 75% of particles fall in the size range 260–360 nm. Therefore the cavitation threshold for 260 nm is experimentally determined as 1.5 MPa. By repeating this process for all experimentally measured probabilities of cavitation at each PRP (and for each of the three particle size ranges), the experimentally determined pressure threshold for each cavity size is superimposed onto the theoretical curve (Fig. 2) at each frequency.

We next determined the duration for which inertial cavitation is sustained by nanocups in a situation where the nuclei are not replenished. Pulsed 0.5 MHz ultrasound was applied to a 6 ml sample volume for 10 min at a pulse repetition frequency of 0.5 Hz and a pressure of 1.2 MPa

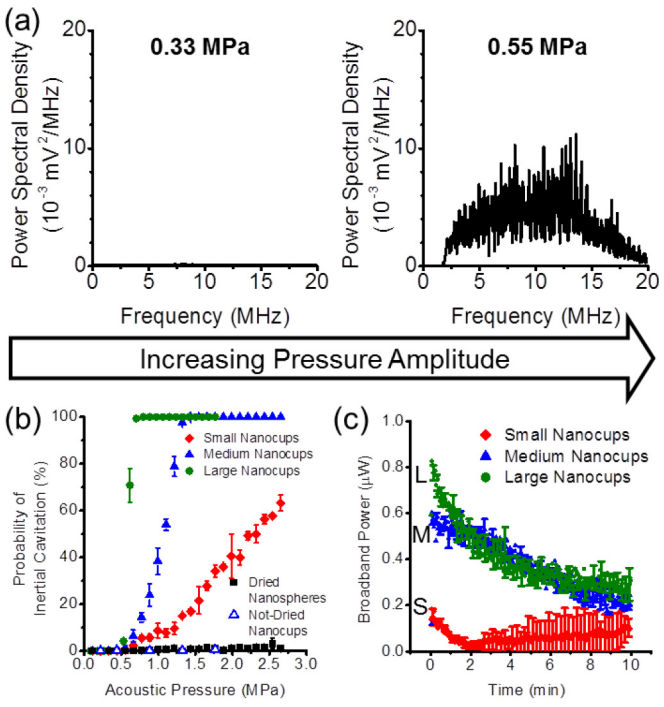

FIG. 4. (Color online) (a) Representative power spectral density curves of medium nanocups exposed to 0.33 MPa and 0.55 MPa pressure amplitudes at 0.5 MHz center frequency. (b) Probability of inertial cavitation curves of nanoparticles exposed to ultrasound at 0.5 MHz. (c) Broadband power of small (S), medium (M), and large (L) nanocups across 10 min of ultrasound exposure. Standard deviations are shown every 60 points for clarity.

with ultrasound parameters previously used by Graham *et al.* [28] for ultrasound-mediated drug delivery. Following the signal processing procedure as above, the resulting broadband energy was determined as a function of time for each nanocup size range [Fig. 4(c)]. The results demonstrate sustained and gradually decaying inertial cavitation activity throughout the 10 min exposure. For comparison, it should be noted that micrometer-sized cavitation nucleation agents, such as microbubbles, are typically depleted in less than 2 min when exposed to the same ultrasound conditions [8].

We believe that the sustained inertial cavitation activity exhibited by our nanocups is due to the increased number density of individual nuclei that lie within the ultrasound focal volume. Only a few nuclei of the right size are necessary to seed inertial cavitation because it is a stochastic process. Furthermore, only a small subset of the nuclei will be excited over a single ultrasonic pulse within the ultrasound focal volume. Therefore, the presence of a nuclei number density that is over two orders of magnitude greater than for microbubbles of equivalent gas fraction will ensure that cavitation is seeded over several more ultrasonic pulses, even if a subset of the nuclei is deactivated upon each exposure.

Following prolonged ultrasound exposure, each size range of nanocups was characterized once again by DLS [Fig. 3(b)]. Each nanocup size range was reduced in mean diameter [Fig. 3(b)] by 10%–20% after ultrasound exposure, suggesting that some material was removed. Post ultrasound TEM images [Figs. 3(b i) and 3(b ii)] evidence no change in shape or morphology. These reductions in the mean size are thus not due to the destruction of the nanocups, but are most probably due to removal of a trapped gas nanobubble.

Prior work [29] has predicted that stable nanobubbles form on hydrophobic surfaces. In order to confirm that successful gas entrapment within the nanocups specifically nucleates inertial cavitation, air-dried smooth polystyrene nanospheres (300 nm) were produced and tested, but found not to yield inertial cavitation at the pressure amplitudes tested [Fig. 4(b)]. We suspect that this lack of response can be attributed to the inability for a sufficiently sized nanobubble to attach on the smooth surface. Furthermore, nanocups that were not air dried also did not induce inertial cavitation [Fig. 4(b)], providing evidence that the preexisting bubble is a necessary requirement. The gradual depletion of cavitation activity [Fig. 4(d)] suggests that there is a depletion of the attached nanobubbles. Collectively, our results demonstrate that trapped bubbles need to lie within the cavity of the nanocup; both the particle shape and entrapment of gas are essential to achieve the observed inertial cavitation effects.

IV. CONCLUSION

In conclusion, by controlling the diameter of nanocavities on nanoparticles, it is possible to tune nanocups that stabilize gas on their surface, dramatically lowering the inertial cavitation threshold of pure water exposed to ultrasound from greater than 30 MPa to as low as 1 MPa. An additional class of nanoparticle cavitation nuclei, i.e., nanocups, were manufactured and characterized. The inertial cavitation thresholds of cavity-size tuned nanocups were initially predicted by a nanocrevice model at two frequencies, and found to agree with experimental measurements. Nanocups produce only broadband signals when exposed to ultrasound, suggesting that only inertial cavitation was nucleated. These acoustic emissions were detected for at least 10 min without nuclei replenishment, which is considerably longer than the 2 min previously documented with microbubbles [8]. Our capability to tune the size and inertial cavitation threshold of nanocups enables the generation of application-specific inertial cavitation nuclei. This is particularly useful for applications such as cancer therapy or sonochemistry, where both particle size and sustainability of cavitation are critical because of the constraints posed by tumor morphology and the range of frequencies and acoustic pressure amplitudes that are safely used.

ACKNOWLEDGMENTS

We thank James Fisk and David Salisbury for manufacturing the various holders and tanks used in this work and Louise Hughes of Oxford Brookes University for her expertise in TEM. The authors gratefully acknowledge financial support from the Centre of Excellence in Personalized Healthcare supported by the Wellcome Trust and the U.K.'s Engineering and Physical Sciences Research Council (EPSRC) under Award No. WT088877/Z/09/Z, from the EPSRC Program Grant (OxCD^3: Oxford Centre for Drug Delivery Devices, Grant No. EP/L024012/1), the RCUK Oxford Centre for Doctoral Training in Healthcare Innovation (Grant No. EP/G036861/1) and the Oxford Clarendon Fund.

[1] T. G. Leighton, *The Acoustic Bubble* (Academic Press, London, 1994).
[2] C. C. Coussios and R. A. Roy, Annu. Rev. Fluid Mech. **40**, 395 (2008).
[3] G. N. Sankin, W. N. Simmons, S. L. Zhu, and P. Zhong, Phys. Rev. Lett. **95**, 034501 (2005).
[4] R. Carlisle, J. Choi, M. Bazan-Peregrino, R. Laga, V. Subr, L. Kostka, K. Ulbrich, C. C. Coussios, and L. W. Seymour, JNCI—J. Natl. Cancer Inst. **105**, 1701 (2013).
[5] H. Chen, W. Kreider, A. A. Brayman, M. R. Bailey, and T. J. Matula, Phys. Rev. Lett. **106**, 034301 (2011).
[6] J. H. Bang and K. S. Suslick, Adv. Mater. **22**, 1039 (2010).
[7] D. F. Rivas, A. Prosperetti, A. G. Zijlstra, D. Lohse, and H. J. G. E. Gardeniers, Angew Chem. Int. Ed. **49**, 9699 (2010).
[8] M. Bazan-Peregrino, B. Rifai, R. C. Carlisle, J. Choi, C. D. Arvanitis, L. W. Seymour, and C. C. Coussios, J. Controlled Release **169**, 40 (2013).
[9] N. Y. Rapoport, A. M. Kennedy, J. E. Shea, C. L. Scaife, and K. H. Nam, J. Controlled Release **138**, 268 (2009).
[10] R. Suzuki, Y. Oda, N. Utoguchi, and K. Maruyama, J. Controlled Release **149**, 36 (2011).
[11] X. Wang *et al.*, Small **10**, 1403 (2014).
[12] S. I. Madanshetty and R. E. Apfel, J. Acoust. Soc. Am. **90**, 1508 (1991).

[13] S. I. Madanshetty, R. A. Roy, and R. E. Apfel, J. Acoust. Soc. Am. **90**, 1515 (1991).
[14] B. M. Borkent, S. Gekle, A. Prosperetti, and D. Lohse, Phys. Fluids **21**, 102003 (2009).
[15] A. A. Atchley and A. Prosperetti, J. Acoust. Soc. Am. **86**, 1065 (1989).
[16] M. A. Chappell and S. J. Payne, J. Acoust. Soc. Am. **121**, 853 (2007).
[17] B. A. Johnson, J. Kreuter, and G. Zografi, Colloids Surf. **17**, 325 (1986).
[18] E. A. Neppiras, Phys. Rep. **61**, 159 (1980).
[19] R. E. Apfel and C. K. Holland, Ultrasound Med. Biol. **17**, 179 (1991).
[20] H. Lv, Q. Lin, K. Zhang, K. Yu, T. J. Yao, X. H. Zhang, J. H. Zhang, and B. Yang, Langmuir **24**, 13736 (2008).
[21] M. Okubo and H. Minami, Colloid Polym. Sci. **275**, 992 (1997).
[22] M. Okubo, H. Minami, and K. Morikawa, Colloid Polym. Sci. **279**, 931 (2001).
[23] S. Graham *et al.*, J. Controlled Release **178**, 101 (2014).
[24] Z. Kyriakou, M. I. Corral-Baques, A. Amat, and C. C. Coussios, Ultrasound Med. Biol. **37**, 568 (2011).
[25] A. D. Maxwell, C. A. Cain, T. L. Hall, J. B. Fowlkes, and Z. Xu, Ultrasound Med. Biol. **39**, 449 (2013).
[26] C. D. Arvanitis, M. Bazan-Peregrino, B. Rifai, L. W. Seymour, and C. C. Coussios, Ultrasound Med. Biol. **37**, 1838 (2011).
[27] K. Yasui, T. Tuziuti, J. Lee, T. Kozuka, A. Towata, and Y. Iida, Ultrason. Sonochem. **17**, 460 (2010).
[28] S. M. Graham *et al.*, J. Controlled Release **178**, 101 (2014).
[29] K. Yasui, T. Tuziuti, W. Kanematsu, and K. Kato, Phys. Rev. E **91**, 033008 (2015).